

# Metrological Characterization of Nuclear Magnetic Resonance Markers for Real-time Field Control of the CERN ELENA Ring Dipoles

Christian Grech, *Student Member, IEEE*, Rachel Avramidou, Anthony Beaumont, Marco Buzio, Nicholas Sammut, *Member, IEEE*, and Jacques Tinembart

**Abstract**—Field markers in particle accelerators are used to provide a digital trigger when the magnetic field reaches a pre-set threshold. This paper describes the results of a test campaign performed on the Extra Low ENergy Antiproton (ELENA) decelerator's main bending dipoles at the European Organization for Nuclear Research (CERN) investigating the behavior of Nuclear Magnetic Resonance (NMR) markers in ramping fields. Following the conclusions of an off-line study using a spare dipole, a series of tests performed on the reference magnet powered in series with the ring showed a NMR signal with a reproducibility better than  $9\ \mu\text{T}$  at field levels lower than 47 mT, using slow ramp rates. This is promising for the real-time field control of the decelerator. For a high-field marker using high ramp rates, the reproducibility of the signal was found to be better than  $3\ \mu\text{T}$ .

**Index Terms**—B-train, magnetic field marker, nuclear magnetic resonance, particle accelerators, real-time magnetic field measurement.

## I. INTRODUCTION

**P**RECISE knowledge of the magnetic field is essential for the optimal operation of a synchrotron particle accelerator. Real-time magnetic field measurement systems are used for radio frequency cavity control, power supply control, beam diagnostics and qualitative feedback to operators. In the superconducting magnets of the Large Hadron Collider (LHC) at the European Organization for Nuclear Research (CERN), measurement-based models describing the dynamic response of the magnet are sufficient as effects related to eddy currents, temperature drifts, material aging and hysteresis are not as significant as in resistive magnets [1]. For the other six synchrotrons including the LHC injector chain, precise

knowledge of the instantaneous total bending field is obtained using the so-called B-train system, where measurements are carried out using a reference magnet powered in series with the ring's magnets.

The B-train field measurement system consists of a static induction coil shaped to follow the nominal beam path. This coil generates a voltage  $V_c$ , proportional to the field time variation, acquired using an analog-to-digital converter. This voltage is integrated using a digital integrator in order to calculate the magnetic field  $B(t)$ . A field marker that triggers a TTL signal at  $t = t_0$  when  $B = B_0$  is then used as an integration constant, as it provides an accurate absolute field value. Magnetic markers are used to improve the B-train's accuracy and reproducibility, as they consider the remanent field and correct the gain and offset drifts of the electronics [2]. The calculation for the average  $B(t)$  is noted in Equation 1 where  $A_c$  refers to the surface area of the coil.

$$B(t) = \frac{1}{A_c} \int_{t_0}^t V_c dt + B_0 \quad (1)$$

In this paper, the behavior of the NMR field marker in dynamic conditions (non-zero ramp rate) using METROLAB's PT2025 teslameter [3] is presented. First, a general overview of different field markers will be presented, followed by the requirements of the B-train system for the ELENA ring. Then, the measurements done on a spare magnet before commissioning are described, where the characteristics of the NMR signal using different ramp rates were investigated for the application in the ELENA B-train. Finally, the tests performed during commissioning, using the reference magnet and the B-train instruments, which investigate the reproducibility of the instrumentation are reported. Whilst systematic errors in the measurement are very difficult to determine, these can be easily compensated for at the operation stage. The main aim of this study is to verify the reproducibility of measurements to be within the specified  $10\ \mu\text{T}$  tolerance, which is very important for the operation of the decelerator, especially at the untested low field limit of the NMR marker (which is around half of the tested field level), where the S/N ratio of the signal is poor ( $\approx 20\ \text{dB}$ ). A secondary objective is to minimize the latency of the measurement, which is part of a regulation loop. The ultimate goal is to allow operation teams flexibility in the use of different magnetic field and ramp rate values due

Manuscript received March 9, 2018; revised April 10, 2018; accepted May 29, 2018. This work has been carried out at CERN in the framework of a scientific collaboration with the University of Malta.

C. Grech is with CERN, European Organization for Nuclear Research, Geneva, Switzerland and with the University of Malta, Malta, e-mail: (christian.grech@cern.ch).

R. Avramidou is with CERN, European Organization for Nuclear Research, 12 Geneva, Switzerland and with the University of Derby, Derby, UK, e-mail: (rachel.avramidou@cern.ch).

A. Beaumont is with CERN, European Organization for Nuclear Research, Geneva, Switzerland and with EPFL, Ecole Polytechnique Federale de Lausanne, Lausanne, Switzerland, e-mail: (anthony.beaumont@cern.ch)

M. Buzio is with CERN, European Organization for Nuclear Research, Geneva, Switzerland, e-mail: (marco.buzio@cern.ch)

N. Sammut is with the Department of Microelectronics and Nanoelectronics, University of Malta, Malta, e-mail: (nicholas.sammut@um.edu.mt).

J. Tinembart is with Metrolab Technology SA, Geneva, Switzerland, email: (tinembart@metrolab.com)

to the experimental nature of CERN's ELENA decelerator. Another novelty aspect with respect to the state of the art is the inclusion of a second dynamic field marker at high level which is used to set the gain correction as accurately as possible.

## II. FIELD MARKER OVERVIEW

The increasing need for improved magnetic field quality in ramped machines has led to advances in the development of magnetic field measurement sensors. The peaking strip [4] is a magnetic marker which was developed at CERN, and has been used as a marker in the CERN Proton Synchrotron (PS) since its commissioning. This sensor's principle of operation is based on that of a fluxgate magnetometer, but adapted for providing trigger signals when the external field crosses a threshold value, thus causing the magnetization to flip. The main benefit of using this transducer is the compatibility with field gradients, improved by reducing its size. However, the heat dissipation in the biasing coil makes the sensor unsuitable for operation above a few mT [5]. Also, these sensors are very difficult to build as they require very specialized manual labor, as they need to be encased in a blow glass capsule to preserve the state of mechanical strain in the magnetic element.

For the B-train system at CNAO (Centro Nazionale Adroterapia Oncologica), a Hall probe is used as field marker to measure the field at the bottom of the cycle [6]. Even if state-of-the-art Hall probes can have a sufficient metrological performance, the need for sophisticated calibration and temperature drift compensation limits their use in a system that must guarantee reliability and stability over a time span of decades [7].

Nuclear Magnetic Resonance (NMR) is a standard for field sensors, providing the best accuracy for a wide magnetic field range [8]. The operating principle of NMR is based on the precession frequency of the proton spin in the nucleus, which varies linearly with the magnetic field amplitude, proportional to a gyromagnetic ratio ( $\gamma = 42.57608$  MHz/T). The commercial NMR equipment is designed to measure quasi-static fields by sweeping the frequency and locking on the occurrence of the resonance curve. The innovative instrumentation aspect of the field marker measurement is the use of a commercial teslameter in marker mode in a changing field, where the NMR probe is excited with a continuous wave at a given frequency by an RF generator. The NMR signal in Figure 1 is generated according to the resonant frequency set and is characterized by the voltage amplitude  $\Delta V$  and the pulse duration  $\Delta t$ .

Several studies [2], [4], [9] were conducted to investigate the use of NMR probes as field markers, with positive results obtained for static DC operation, when placed on field-current plateaus. NMR field markers working simultaneously with the induction coil measurement have already been used to measure with high precision the field in the CERN Super Proton Synchrotron cycle with plateaus at 60 mT and 2 T, but these are not in use anymore [8]. Such field markers are, however, still operational in the PS Booster at CERN,

marking at 110.8 mT in dynamic mode, just before injection. The main limitations of NMR markers are that they cannot be used for fields lower than 43 mT, and the S/N ratio and the width of the resonance signal are degraded by large space and time gradients, as well as very low fields. This limitation is imposed by the type and size of the sample inside the probe. The performance degrades in inhomogeneous fields because the spin in different regions of the probe resonates at different times. In the case of a high space gradient, the system cannot lock the absorption frequency and a compensation coil has to be included [10]. For ramping fields, in [9], it was confirmed that for the PS combined-function magnets, the lower the ramp rate, the better the reproducibility, with the optimal NMR signal obtained at 25.6 mT/s. However, this study cannot be applied directly to the ELENA B-train due to the difference in field uniformity between the ELENA and PS magnets as well as the difference in field levels.

## III. ELENA B-TRAIN REQUIREMENTS

ELENA is a 30 m circumference synchrotron whose aim is to decelerate anti-protons delivered by the Antiproton Decelerator (AD), from 5.3 MeV down to 100 keV and to increase the number of trapped anti-protons. The ELENA ring will hence be operated at an unusually low energy for a synchrotron with a magnetic focusing structure [11]. Obtaining a good magnetic field quality is challenging, due to the very low magnetic fields required and remanence and hysteresis effects. In fact, one of the biggest challenges in real-time magnetic measurement is the extremely low ejection field of 50 mT, where the beam line is vulnerable to external field perturbation due to electric lines and other elements. The most stringent requirements for the ELENA B-train include a measurement reproducibility of 10  $\mu$ T at low-field, and a total cycle length up to 120 s, which may cause a build-up of errors such as integrator drift. The complete specifications for the ELENA B-train are listed in Table I.

Figure 2 shows an example of the placement of the field

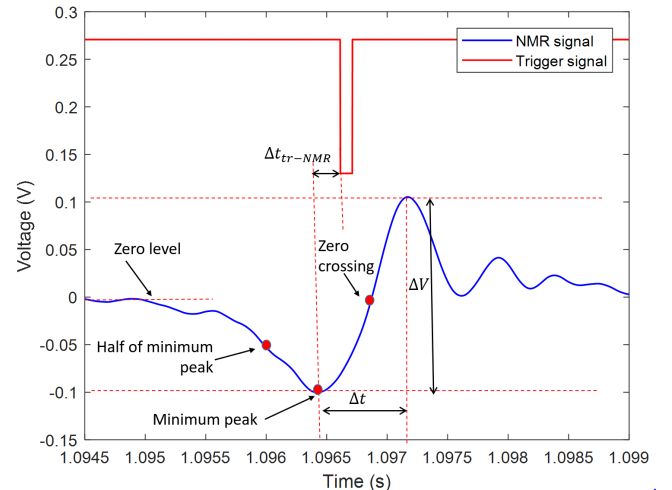


Fig. 1. The NMR output and the resulting trigger signal (scaled)

TABLE I  
THE ELENA B-TRAIN SPECIFICATIONS [12]

Parameter	Value
Minimum magnetic field in the gap (mT)	45
Maximum magnetic field in the gap (mT)	420
Minimum ramp duration (s)	1
Measurement reproducibility ( $\mu T$ )	10
Absolute measurement uncertainty ( $\mu T$ )	25
Nominal field-current relation (mT/A)	1.313

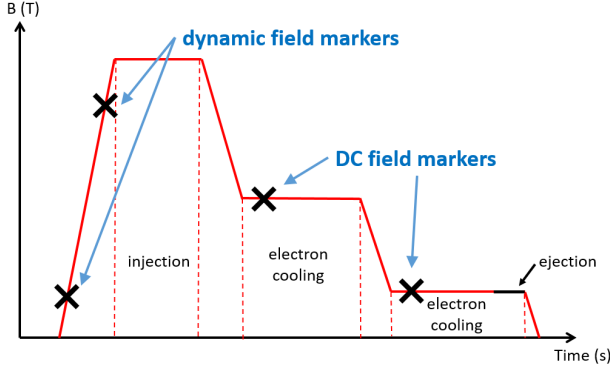


Fig. 2. Field marker placement along the ELENA decelerating cycle

markers along the ELENA decelerating cycle for two different operation modes. The ELENA ring can also be used in accelerating mode, where the injection level is at 45 mT. This restricts the lower field marker to a field level lower than 45 mT. In dynamic mode, the NMR probe creates a trigger every time the field crosses a preset value, while in DC mode, the Teslometer produces a timing trigger and accepts a  $\mu T$ -accurate measurement given that the field is sufficiently stable. The number of field markers at different levels depends on the metrological performance of the whole system, and each marker can perform up to two drift and gain corrections per cycle [12].

#### IV. OFFLINE MEASUREMENTS

##### A. Experimental Setup

The setup consisted of the ELENA spare dipole PXMBHEKCWP-DA000002, equipped with a nine-coil litz-wire fluxmeter for the magnetic field measurement, via the integrated induced voltage to its central coil. A PT2025 NMR teslometer by Metrolab with a resolution of  $0.1 \mu T$  and a nominal accuracy of 5 ppm was used for generating the NMR signal. The complete experimental setup is shown in Figure 3.

Four NMR probes for different magnetic ranges were used: Probe 1 (0.043 T - 0.13 T), Probe 2 (0.09 T - 0.26 T), Probe 3 (0.17 T - 0.52 T) and Probe 4 (0.35 T - 1.05 T). The probes consist of the measuring head and the NMR detection circuit, which can be connected to the NMR Teslometer by a  $50 \Omega$  coaxial cable and a screened cable with two wires for modulation. A CERN-made power supply, Apolo [13], and a Direct Current-Current Transformer for the current measurement were used. A 50 MHz Aim-TTi Function/Pulse

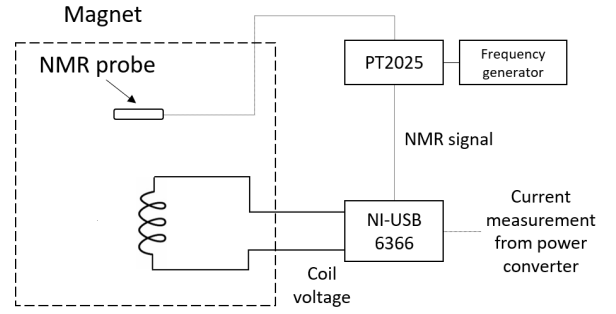


Fig. 3. The experimental setup for the offline measurements

Generator [14] connected to the NMR probe was used for the fixed RF excitation frequency in the MHz range, in order to measure pulsed magnetic fields. Measurement of the central coil voltage, the electric current and the NMR signal were acquired and recorded using a National Instruments (NI) USB card (USB-6366).

##### B. NMR signal interpretation

The purpose of these measurements was to compare different methods for the dynamic measurement of the magnetic field using the NMR signal. The final aim was to choose an arbitrary reference point for the transient resonance in the sample of the NMR probe. The measurement procedure involved ramping up the magnet several times from 37.93 A to 326 A at 300 A/s, using a NMR signal as an absolute measurement at DC. The NMR signal in dynamic mode was detected before the end of the ramp up, and the corresponding relative magnetic field noted at three different points using the central induction coil. The three different approaches considered were (see Figure 1) using the half value between the minimum peak and the zero level (Method 1), using the minimum peak of the NMR signal (Method 2) and using the zero crossing of the NMR signal (Method 3). Once these time instances were detected, the corresponding value of the magnetic field was derived.

Since the NMR output fluctuates slowly, the baseline level obtained by averaging the signal between resonance transients was subtracted. Table II summarizes the results of the measurements, which involved 9 repetitions each. The column  $\Delta B$  lists the average of the measured relative field over the 9 repetitions, while St. Dev. shows the standard deviation (jitter) of  $B_1$ . These two measurements are depicted in Figure 4. Finally, the column Relative Error illustrates the ratio of the standard deviation to the average magnetic field. Results show that the three methods differ at most by  $100 \mu T$ , while they all have a good repeatability of less than  $10 \mu T$ . The second method was chosen for subsequent measurements because it can easily be implemented with the existing peak detection hardware.

##### C. Effect of ramp rate on voltage difference and time delay

The next series of the measurements studied the characteristics of the NMR signal and more specifically the voltage difference

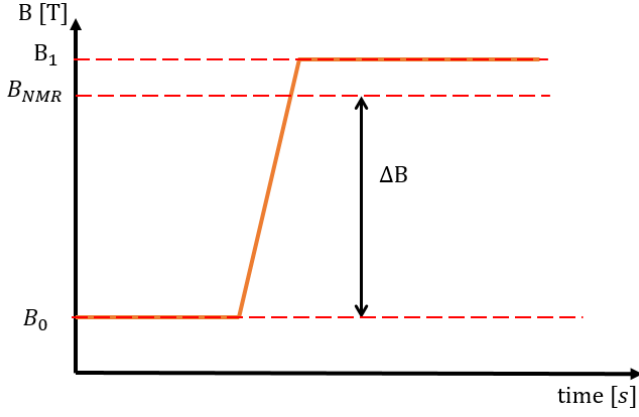


Fig. 4. Parameters involved for the NMR signal interpretation

TABLE II  
METHOD COMPARISON FOR THE MAGNETIC FIELD MEASUREMENTS

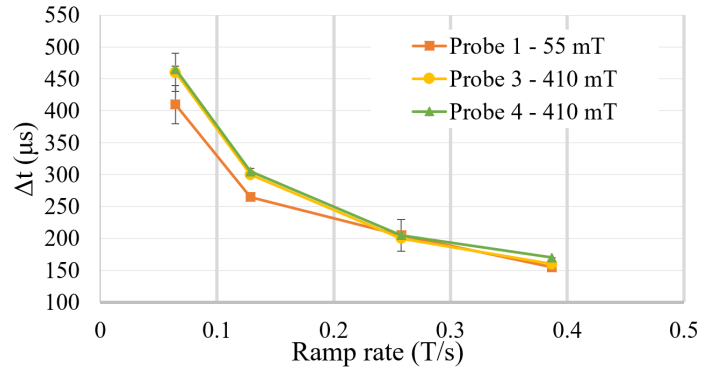
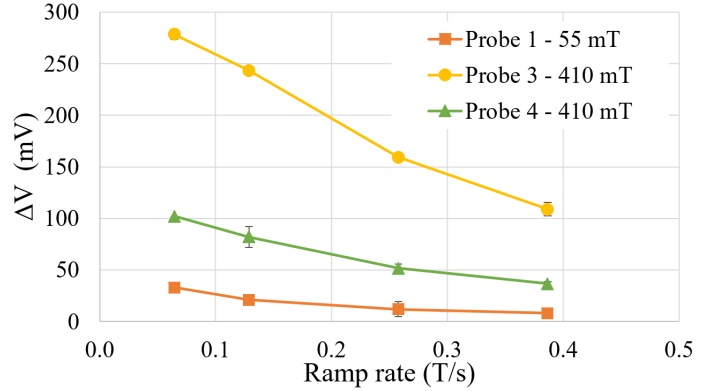
Method	$\Delta B$ (T)	St. Dev. ( $\mu$ T)	Rel. Error ( $\times 10^{-6}$ )
1. Half of minimum peak	0.390929	3.0	7.7
2. Minimum peak	0.390974	2.7	6.8
3. Zero crossing	0.391023	2.5	6.3

$\Delta V$ , as well as the time difference  $\Delta t$  between the two first peaks of the signal, as shown in Figure 1. First, the influence of the ramp rate, the magnetic field and the reproducibility were quantified. Measurements of the amplitude  $\Delta V$  and the pulse duration  $\Delta t$  were taken at different ramp rates and different magnetic fields covering the range from 50 mT to 420 mT, by using the NMR probes 1 (50 mT - 55 mT) and 3 (200 mT - 420 mT). The pulse generator was tuned to the frequency  $f$  that is defined by  $\gamma$  and the magnetic field  $B$ , according to the formula  $f = \gamma B$  and it was connected to the NMR probe. The conclusions were:

- The pulse duration  $\Delta t$  increases for lower ramp rate  $\dot{B}$ . This is intuitive as the field level is reached and exceeded in a slower manner.
- For the same ramp rate  $\dot{B}$ , the pulse duration  $\Delta t$  increases slightly with the magnetic field and it has a lower dispersion at higher ramp rates  $\dot{B}$ .
- The amplitude  $\Delta V$  increases for lower ramp rate  $\dot{B}$
- For the same ramp rate  $\dot{B}$ , the amplitude  $\Delta V$  increases with the magnetic field  $B$ .

Subsequent measurements were focused on magnetic fields of 55 mT and 410 mT (good candidates for the marker mode) for the ramp rates 64 mT/s, 129 mT/s, 258 mT/s and 387 mT/s for the corresponding Probes 1, 3 and 4. In this series of measurements the aim was the comparison of the Probes 3 and 4, as according to the information provided by Metrolab, Probe 3 (170 mT - 520 mT) is expected to provide a stronger NMR signal compared to Probe 4 (350 mT - 1050 mT), because the measured magnetic fields lie in the upper part of its range [3].

The conclusions from this investigation were identical to those

Fig. 5. The pulse duration  $\Delta t$  as a function of the ramp rate for different magnetic fieldsFig. 6. The amplitude  $\Delta V$  as a function of the ramp rate for different magnetic fields

in the previous study with the pulse duration  $\Delta t$  having a lower dispersion at higher ramp rates  $\dot{B}$ , while there was no significant difference between Probes 3 and 4 (Figure 5) while for the amplitude  $\Delta V$ , Probe 3 was noted to perform better compared to Probe 4 (Figure 6).

#### D. Investigating different $B/\dot{B}$ combinations

In another study, the most suitable ratios  $B/\dot{B}$  were tested, with the aim being to select the ratio, which gives a NMR signal with a short pulse duration  $\Delta t$ , and a high amplitude  $\Delta V$ . The results of this series of measurements are included in Table III and are plotted in Figures 7 and 8, in which one can distinguish three groups of points. The first one (blue) corresponds to Probe 1, the second (orange) to Probe 2, while the third one (gray) to Probe 4.

From the results, it can be observed that the best choice in terms of pulse amplitude  $\Delta V$  (above 500 mV) are the lower ramp rates, but in this case the pulse duration  $\Delta t$  is higher (above 210  $\mu$ s). The choice of the ramp rate of 0.38 T/s for magnetic fields 400 mT - 420 mT is a good compromise ( $1 < B/\dot{B} < 1.1$ ) in terms of pulse amplitude  $\Delta V$  (325 mV - 375 mV, marked in green in Figure 7), while the pulse duration  $\Delta t$  is kept at lower levels (150  $\mu$ s - 170  $\mu$ s, marked in green in Figure 8), and the standard deviation is much better. We remark that this optimization is intended to guide

TABLE III  
NMR SIGNAL DEPENDENCE ON THE RATIO  $B/\dot{B}$  FOR VARIOUS COMBINATIONS OF  $B$  AND  $\dot{B}$

Probe no.	$B$ (mT)	$\dot{B}$ (mT/s)	$B/\dot{B}$ (s)	$\Delta V$ (mV)	$\sigma_{\Delta V}$ (mV)	$\Delta t$ ( $\mu$ s)	$\sigma_{\Delta t}$ ( $\mu$ s)
1	50	387	0.13	173	8	160	< 1
1	55	387	0.14	207	3	163	5
1	50	258	0.19	289	2	197	5
1	55	258	0.21	324	13	197	5
1	50	129	0.39	551	16	287	5
1	55	129	0.42	612	15	277	5
2	200	387	0.52	149	4	147	9
2	220	387	0.57	184	14	157	5
2	250	387	0.65	215	18	157	5
4	420	515	0.82	271	7	140	< 1
4	<b>400</b>	<b>387</b>	<b>1.03</b>	<b>329</b>	<b>3</b>	<b>170</b>	< 1
4	<b>410</b>	<b>387</b>	<b>1.06</b>	<b>349</b>	<b>4</b>	<b>170</b>	< 1
4	<b>420</b>	<b>387</b>	<b>1.09</b>	<b>372</b>	<b>6</b>	<b>167</b>	<b>5</b>
4	420	258	1.63	554	4	210	< 1
4	420	129	3.26	544	3	210	< 1
4	420	64	6.52	1070	11	455	5

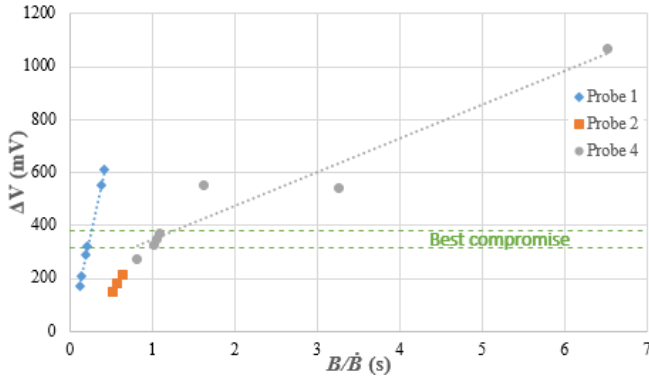


Fig. 7. NMR signal amplitude  $\Delta V$  as a function of the ratio  $B/\dot{B}$

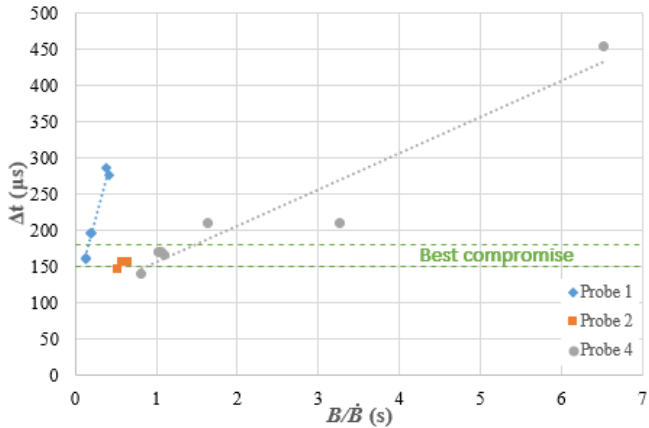


Fig. 8. NMR pulse duration  $\Delta t$  as a function of the ratio  $B/\dot{B}$

the operation team in the fine tuning of magnetic cycles, which evolve constantly during the commissioning and exploitation phases of a synchrotron.

## V. ONLINE COMMISSIONING TESTS

As part of the ELENA ring's commissioning process, the performance of the NMR low-field and high-field markers for

the installed B-train was evaluated. These tests were carried out several months after the offline tests and hence more information was available on the ramp rates of the magnetic cycle and the possible field levels for the NMR markers. The aim of these tests was to validate the choice of the NMR marker field levels, especially the one at low-field, which had to be set at the lower limit of Probe 1's range, due to a low injection level of 45 mT when particles in the ELENA ring are accelerated. Furthermore, these tests were also aimed at validating the performance of the B-train's peak detection card, which detects the minimum peak of the NMR signal and provides a trigger signal  $t_0$ , when the NMR markers reading is  $B = B_0$  (see Figure 1).

### A. Experimental Setup

In this case, the ELENA reference dipole PXMBHEKCWP-DA000001, was used for the tests, with the magnetic field measurements carried out using the PT2025 NMR teslameter by Metrolab and NI USB card (USB-6366) with an acquisition rate of 1 MHz. Probe 1 was used for the low-field measurements while Probe 3 was used at the high-field mark. For all tests, the performance of four identical NMR teslameters was compared. These are part of two separate B-train systems: the operational (OP) system, which is used during normal operation and the spare (SP) system, which is used for testing purposes, as well as a backup. A separate peak detection card was used for each NMR signal in order to generate a trigger signal. The complete setup is illustrated in Figure 9.

Following the outcomes of the offline study and more insight on the possible ELENA machine cycles, twelve  $(B, \dot{B})$  cases were considered, with more focus on the low-field marker, due to the bigger challenges that a marker at this level presents. Five different ramp rates were tested for the low-field marker, while the high-field marker was tested at three different ramp rates. Figure 10 shows the different combinations of  $B$  and  $B/\dot{B}$  considered, as well as the two operating points for the markers as they were used during the commissioning of the decelerator.



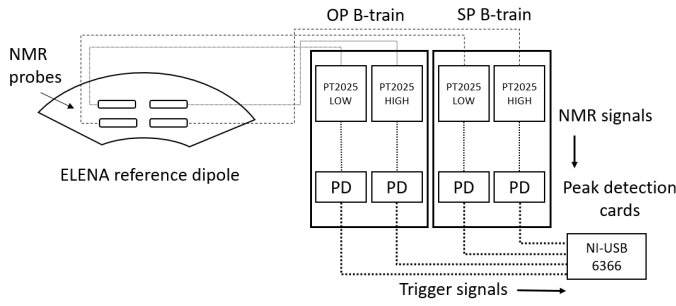
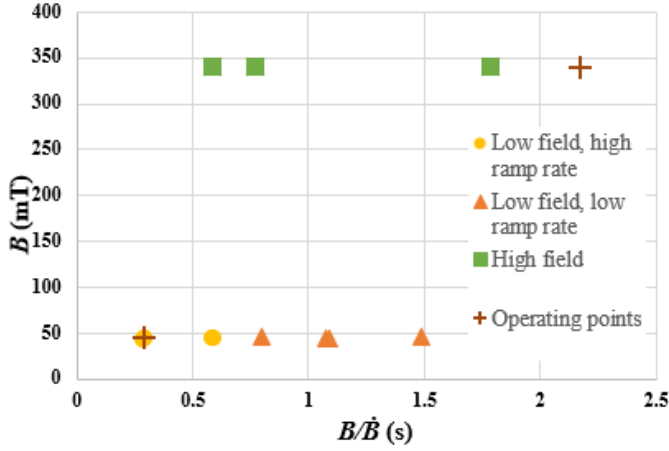


Fig. 9. The experimental setup for the online measurements

Fig. 10. The different  $B$  and  $B/\dot{B}$  combinations considered and the operating points

The NMR probe includes a bandpass filter from 100 Hz to 2 kHz, which is however insufficient to guarantee the quality of the signal due to the high electrical noise levels in the ELENA powerhouse, where the system is located. To reduce the possibility of spurious peak detection, an additional low-pass filter with a 2.3 kHz cutoff was applied at the acquisition end. The effect of this filter on the time location of the peak was measured to be about 62  $\mu$ s, which adds up to the delay of about 100  $\mu$ s due to the in-built filter. At the operational field ramp rates, the total delay does not exceed 80  $\mu$ s. Being systematic, this delay can be compensated in operation and has been ignored in the analysis that follows. In practice, what counts is the stability of these filters, which may impact the jitter of the detected peak.

### B. Required Uniformity of the Field

The uniformity of the field for the ELENA dipole was compared to the specifications for the PT2025 teslameter. When the field is not uniform, one side of the sample resonates at a different frequency from the other side. As the gradient increases the resonance peak broadens and flattens, disappearing in the noise. The limits recommended by the manufacturer are 600 ppm/cm at low field and 1400 ppm/cm at high field. The uniformity of the field was measured to be 130 ppm/cm at 100 A and 400 A during the series test campaign [15], which is well within the limit in both cases.

### C. Trigger signal precision

The B-train system provides a trigger signal  $t_0$  when the NMR output signal reaches its negative minimum value. The trigger signal corresponds approximately to the moment when the field  $B$  matches the NMR resonance frequency but includes the effect of the electronics, both the RF demodulator in the teslameter and the FPGA peak detector. This small difference, investigated in Section V-D, has mostly a systematic character and does not impact operation. Figure 11 shows the NMR signals recorded using the operational system at 46.5 mT and 58 mT/s. Following the analysis of 100 signals for the ten different  $(B, \dot{B})$  parameter combinations, the repeatability ( $1\sigma$ ) of the trigger signal generation  $\sigma_{t_{NMR}}$  was found using the standard deviation of the trigger time. Comparison of subsequent cycles requires the assumption that the magnetic history is repeatable as a function of time after ignoring the first few magnetic cycles. This was verified independently, where measurements made on a spare magnet showed that at least three precycles are needed to achieve a stable hysteresis loop. Furthermore, the equivalent value in tesla  $\sigma_{B(t_{NMR})}$  was calculated by multiplying  $\sigma_{t_{NMR}}$  by the ramp rate. Finally, the relative standard deviation with respect to  $B$  ( $\sigma_{B(t_{NMR})}/B$ ) was calculated, in order to compare the performance with the reproducibility target of 10  $\mu$ T.

The results can be seen in Table IV, which shows the results obtained for three cases labeled low field, high ramp rate (in yellow); low field, low ramp rate (in orange); and high field (in green). We can see that lower ramp rates are more desirable for lower standard deviations at low field. The reproducibility of the trigger signal for  $B/\dot{B} > 0.8$  s was calculated to be better than 4.5  $\mu$ T ( $1 \times 10^{-4}$ ), while for faster ramp rates, it was better than 9  $\mu$ T ( $2 \times 10^{-4}$ ), both of which are below the targeted 10  $\mu$ T. At high field, a reproducibility of 3  $\mu$ T ( $0.09 \times 10^{-4}$ ) was noted, below the 10  $\mu$ T specification, which was expected, due to the high S/N ratio of the signal at this range.

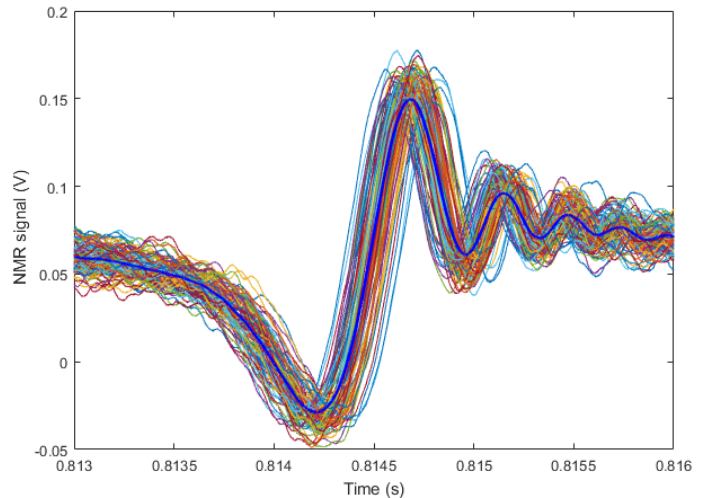


Fig. 11. NMR signals obtained using OP system at 46.5 mT and 58 mT/s, with the average signal shown in blue.

TABLE IV  
TRIGGER SIGNAL REPEATABILITY FOR VARIOUS COMBINATIONS OF  $B$  AND  $\dot{B}$

Probe no.	$B$ (mT)	$\dot{B}$ (mT/s)	$B/\dot{B}$ (s)	$\sigma_{t_{NMR}}$ [ms]		$\sigma_{B(t_{NMR})}$ [ $\mu$ T]		$\sigma_{B(t_{NMR})}/B$ [ $10^{-4}$ ]	
				OP	SP	OP	SP	OP	SP
1	43.0	151	0.284	0.037	0.036	5.6	5.5	1.30	1.28
1	44.5	151	0.294	0.047	0.047	7.1	7.1	1.60	1.60
1	45.0	151	0.297	0.054	0.059	8.2	9.0	1.82	2.00
1	44.5	76	0.588	0.063	0.062	4.8	4.7	1.08	1.06
1	45.0	76	0.594	0.075	0.075	5.7	5.7	1.27	1.27
1	46.5	58	0.800	0.057	0.055	3.3	3.2	0.71	0.69
1	44.5	41	1.077	0.067	0.065	2.8	2.7	0.63	0.61
1	45.0	41	1.090	0.104	0.109	4.3	4.5	0.96	1.00
1	46.5	31	1.490	0.108	0.099	3.4	3.1	0.73	0.67
3	340	584	0.582	0.0039	0.0044	2.3	2.6	0.07	0.08
3	340	443	0.767	0.0056	0.0067	2.5	3.0	0.07	0.09
3	340	195	1.744	0.0138	0.0137	2.7	2.7	0.08	0.08

TABLE V  
DELAY BETWEEN NMR MINIMUM PEAK AND TRIGGER SIGNAL

$B$ (mT)	$\dot{B}$ (mT/s)	$B/\dot{B}$ (s)	$\Delta t_{tr-NMR}$ [ms]		$\sigma_{\Delta t_{tr-NMR}}$ [ms]		$\Delta B_{tr-NMR}$ [ $\mu$ T]		$\sigma_{\Delta B_{tr-NMR}}$ [ $\mu$ T]		$\sigma_{\Delta B_{tr-NMR}}/B$ [ $10^{-4}$ ]	
			OP	SP	OP	SP	OP	SP	OP	SP	OP	SP
43.0	151	0.284	0.108	0.120	0.057	0.055	16.4	18.1	8.6	8.3	2.00	1.93
44.5	151	0.294	0.117	0.127	0.070	0.067	17.8	19.2	10.7	10.1	2.40	2.27
45.0	151	0.297	0.122	0.149	0.078	0.086	18.4	22.5	11.8	13.0	2.62	2.89
44.5	76	0.588	0.133	0.153	0.089	0.092	10.1	11.6	6.7	6.9	1.51	1.55
45.0	76	0.594	0.136	0.166	0.106	0.106	10.3	12.6	8.1	8.0	1.80	1.78
46.5	58	0.800	0.109	0.120	0.082	0.079	6.4	7.0	4.8	4.6	1.03	0.99
44.5	41	1.077	0.141	0.160	0.095	0.096	5.8	6.6	3.9	3.9	0.88	0.88
45.0	41	1.090	0.169	0.191	0.150	0.157	7.0	7.9	6.2	6.5	1.38	1.44
46.5	31	1.490	0.140	0.149	0.109	0.136	4.4	4.6	4.8	4.2	1.03	0.90
340	584	0.582	0.009	0.009	0.005	0.006	5.4	5.1	3.2	3.7	0.09	0.11
340	443	0.767	0.010	0.010	0.008	0.009	4.6	4.5	3.5	4.2	0.10	0.12
340	195	1.744	0.013	0.013	0.020	0.019	2.6	2.5	3.8	3.7	0.11	0.11

#### D. Delay of trigger signal generation

Another test carried out was the measurement of the time difference  $\Delta t_{tr-NMR}$  between the minimum peak of the original NMR signal (i.e. unfiltered) and the falling edge of the trigger signal (active low), as shown in Fig. 1. This delay was measured with a resolution of 1  $\mu$ s. Table V shows the delay in seconds and in tesla ( $\Delta B_{tr-NMR}$ ), as well as its standard deviation in seconds ( $\sigma_{\Delta t_{tr-NMR}}$ ) and in tesla ( $\sigma_{\Delta B_{tr-NMR}}$ ), and finally relative to  $B$  ( $\sigma_{\Delta B_{tr-NMR}}/B$ ). The standard deviation of the delay is larger than the standard deviation of the trigger, which proves that filtering takes effectively away noise that would otherwise perturb the measurement. The standard deviation of the delay increases with ramp rate, which confirms the result obtained in the previous test. One also has to note that this delay does not include the systematic contribution due to the NMR probe's in-built filter.

#### E. Conclusion

The main outcome of this study can be summarized as follows:

- Using the minimum peak of the NMR signal to derive the magnetic field always produces results with a repeatability better than the B-train target 10  $\mu$ T. Low-pass filtering is essential to achieve this performance.
- The most critical conditions are at low field, where the ramp rate should be kept as low as possible. At field levels

lower than 47 mT, a reproducibility better than 4.5  $\mu$ T was found using slow ramp rates ( $B/\dot{B} > 0.8$  s), while for faster ramp rates, it was better than 9  $\mu$ T.

- For a high-field marker using a high ramp rate, the reproducibility was found to be better than 3  $\mu$ T.
- For high field (400 mT - 420 mT), using a high ramp rate of 387 mT/s is a good compromise for voltage amplitude, pulse duration and repeatability.
- The pulse duration and the amplitude of the NMR signal both increase for lower ramp rates. Hence, a compromise must be met to have a large voltage amplitude, with a reasonable pulse duration.
- Using Probe 3 as a marker in fields lower than 410 mT is more beneficial for a stronger NMR signal than using Probe 4 for the same range.
- For low fields, it was noticed that lower ramp rates result in larger NMR voltage amplitude signals, however at the expense of a higher pulse duration (latency) and jitter. A compromise should be reached in this case, between the two extremes.
- The homogeneity of the ELENA reference magnet field at the chosen low and high field values satisfies the maximum field gradient accepted for the two PT2025 Teslameter probes tested.

The Metrolab NMR probe is found to be fully adequate

to be used as a high-precision field marker for the real-time field measurement systems of the ELENA ring, which operates at low energies and hence low magnetic fields. This characterization process is important as it can define what can and cannot be done when cycling the magnets. Further tests will be performed in the future to compare NMR markers to ferrimagnetic resonance markers. If needed, the stability of both internal and external NMR signal filters could be improved by implementing high-precision components less sensitive to temperature variations.

#### ACKNOWLEDGMENT

The authors would like to thank CERN colleagues Martino Colciago, David Giloteaux, Daniel Oberson and Marco Roda for their contribution to the B-train system, as well as Lucio Fiscarelli, Carlo Petrone for fruitful discussions.

#### REFERENCES

- [1] N. Sammut, L. Bottura, and J. Micallef, "Mathematical formulation to predict the harmonics of the superconducting Large Hadron Collider magnets," *Phys. Rev. ST Accel. Beams*, vol. 9, p. 012402, Jan 2006.
- [2] F. Caspers and D. Cornuet, "NMR Probe as a Field Marker in a Quadrupole," *Eleventh International Magnet Measurement Workshop (IMMW)*, 09 1999.
- [3] *PT2025 NMR Teslameter User Manual*, 2nd ed., METROLAB Instruments SA, Sep. 2003.
- [4] M. Benedikt, F. Caspers, and M. Lindroos, "Application of magnetic markers for precise measurement of magnetic fields in ramped accelerators," *Particle Accelerators*, no. 63, 1999.
- [5] J. M. Kelly, "Magnetic Field Measurements with Peaking Strips," *Review of Scientific Instruments*, vol. 22, no. 4, pp. 256–258, 1951.
- [6] G. Franzini *et al.*, "Final Design and Features of the B-train System of CNAO," *IPAC*, 2010.
- [7] G. Golluccio *et al.*, "Metrological performance of a ferrimagnetic resonance marker for the field control of the CERN Proton Synchrotron," *IEEE Trans. on Applied Superconductivity*, vol. 22, no. 3, June 2012.
- [8] C. Reymond, "Magnetic Resonance Techniques," in *CERN Accelerator School: Measurement and Alignment of Accelerator and Detector magnets*, S. Turner, Ed. CERN, 1998, pp. 219–232.
- [9] A. Beaumont, "Magnetic field markers of the B-Train for the Proton Synchrotron accelerator," CERN, Tech. Rep., 2008.
- [10] G. Golluccio *et al.*, "Static metrological characterization of a ferrimagnetic resonance transducer for real-time magnetic field markers in particle accelerators," in *2011 IEEE Instrumentation and Measurement Tech. Conference*, May 2011.
- [11] W. Bartmann *et al.*, "Extra Low Energy Antiproton Ring ELENA: from the Conception to the Implementation Phase," *IPAC*, 2014.
- [12] V. Chohan *et al.*, "ELENA Design Report," Available: <https://cds.cern.ch/record/2235240>, 2016.
- [13] *APOLLO Documentation*, CERN, available: <https://section-mpc.web.cern.ch/content/documentation-apollo>.
- [14] *Aim-TTi TF930*, Thandar Thurlby Instruments, available: <http://docs-europe.electrocomponents.com/webdocs/0d08/0900766b80d084a0.pdf>.
- [15] R. Chritin *et al.*, "Results of Magnetic Measurement Tests on the Full-Scale Straight Prototype of ELENA Dipole," CERN, Tech. Rep., 2015. [Online]. Available: <https://edms.cern.ch/ui/file/1381410/1.0/LNA-MBHEK-TR-0001-10-00.pdf>



**Christian Grech** (S'14) received the B.Eng.(Hons) degree in electrical and electronics engineering from the University of Malta in 2016, where he is currently pursuing a Ph.D. degree. He is actively participating in a collaboration between the Department of Microelectronics and Nanoelectronics and the Magnetic Measurement section at CERN, carrying out research on magnetic modeling, system identification and magnetic measurements. His main research interests concern signal processing, instrumentation and mathematical modeling.



**Rachel Avramidou** received a Bachelor degree in Physics from the Physics Department and a M.Sc. degree in Microelectronics Engineering (VLSI design) from the Department of Informatics and Telecommunications of the National University of Athens. She received a second M.Sc. in Physics and its Technological Applications and a PhD in Applied Physics from the School of Applied Sciences of National Technical University of Athens, having carried out research with the ATLAS Collaboration at CERN, with specialization in detector instrumentation. Her main research interests are in the field of detector and accelerator instrumentation and their electronics. She worked with the Magnetic Measurement section at CERN as a project associate representing the University of Derby, where she holds a visiting Professorship.



**Anthony Beaumont** received the M.Sc. in Electrical Engineering from the University of Belfort Montbéliard (FR) in 2009. Since 2010 he has been at CERN, where he has been in charge of magnetic measurements for different projects, including the renovation of the B-train systems and a collaboration with the hadron therapy center MedAustron. He is currently pursuing a Ph.D. degree at the EPFL, Lausanne (CH) on magnetic field sensors.



**Marco Buzio** received a M.Sc. in Aerospace Engineering in 1992 from the Polytechnic of Milan (IT) and a Ph.D. in Computational Mechanics in 1998 from the Imperial College, London (UK). He worked on electromechanical computer models at the JET tokamak (Abingdon, UK) and is since 1998 at CERN, where he is Senior Engineer in the field of magnets for particle accelerators. He is in the organizing board of the International Magnetic Measurement Workshop. His research interests include magnetic field metrology, modeling and control of

hysteretic and fast-pulsed magnetic devices and inverse techniques for the current distribution in superconducting magnets.



**Nicholas Sammut** received the B.Eng. (Hons) degree in electrical engineering, the M. Ent. degree in entrepreneurship and the Ph.D. in electrical engineering from the University of Malta. His Ph.D. research on the Field Description of the Large Hadron Collider was carried out with the Magnetic Measurements and Tests Group at CERN. Since 2007, he was an academic in the department of Microelectronics and Nanoelectronics at the University of Malta. He also serves as deputy dean of the Faculty of Information and Communications Technology of the same university. He served as a board member of several Maltese, European and International organizations and committees. His main research interests are in the field of accelerator technology, sensors, instrumentation and measurement.



**Jacques Tinembart** received the M.Eng. degree in electrical engineering from the École polytechnique fédérale de Lausanne (EPFL). Before joining Metrolab Technology SA (Switzerland) in 2007, he worked as Professor at the University of Applied science, HES-SO, Geneva. His research is focused on developing state of the art magnetometers using the NMR, Hall and Integrator techniques.